Biochimica et Biophysica Acta 1822 (2012) 1147–1153

Contents lists available at SciVerse ScienceDirect

Biochimica et Biophysica Acta

journal homepage: www.elsevier.com/locate/bbadis

Quantitative magnetic analysis reveals ferritin-like iron as the most predominant iron-containing species in the murine Hfe-haemochromatosis

Lucía Gutiérrez [a,b,*,1], Maja Vujić Spasić [c,**,1], Martina U. Muckenthaler [c], Francisco J. Lázaro [d]

[a] School of Physics, M013, The University of Western Australia, 6009, Crawley, Australia
[b] Instituto de Ciencia de Materiales de Madrid, ICMM-CSIC, Cantoblanco 28049, Madrid, Spain
[c] University Hospital of Heidelberg, Department of Hematology, Immunology and Oncology and Molecular Medicine Partnership Unit, 69120, Heidelberg, Germany
[d] Departamento de Ciencia y Tecnología de Materiales y Fluidos, Universidad de Zaragoza, 50018, Zaragoza, Spain

ARTICLE INFO

Article history:
Received 9 December 2011
Received in revised form 1 March 2012
Accepted 13 March 2012
Available online 20 March 2012

Keywords:
Ferritin
Iron
AC susceptibility
Paramagnetic
Hfe
Haemochromatosis

ABSTRACT

Quantitative analysis of the temperature dependent AC magnetic susceptibility of freeze-dried mouse tissues from an Hfe hereditary haemochromatosis disease model indicates that iron predominantly appears biomineralised, like in the ferritin cores, in the liver, the spleen and duodenum. The distribution of the amount of ferritin-like iron between genders and genotypes coincides with that of elemental iron and nonheme iron. Importantly, the so-called paramagnetic iron, a quantity also determined from the magnetic data and indicative of nonmineralised iron forms, appears only marginally increased when iron overload takes place.

1. Introduction

Iron is an essential element required for redox processes in all eukaryotes and most prokaryotes. As an atom, iron has the capacity to accept and donate electrons readily, interconverting between ferric (Fe^{3+}) and ferrous (Fe^{2+}) forms. This property makes iron a useful component of cytochromes, oxygen-binding molecules (such as haemoglobin and myoglobin) and a variety of enzymes. However, due to its potency to generate reactive oxygen species, free iron is toxic and thus nearly all of the iron in the body is stored or complexed into ferritin, haemoglobin or transferrin proteins [1].

In the search for analytical techniques to determine different iron forms in tissues of patients with iron-related diseases, the magnetic properties of this element have long attracted attention [2]. It was known quite early that deoxyhaemoglobin, methaemoglobin and myoglobin exhibit a measurable magnetic susceptibility (the magnetisation of the sample divided by the magnitude of an externally applied magnetic field) whose origin resides on the single ion magnetism of Fe^{2+} or Fe^{3+} incorporated within the prosthetic groups of their molecules [3–5]. This magnetic behaviour is called *paramagnetic* and can be identified by measuring the static magnetic susceptibility χ whose temperature dependence follows the Curie law $\chi = C/T$, where C is a constant and T is the absolute temperature. The magnetic behaviour of the iron ions does also depend on their atomic environment in the molecule in such a way that, e.g., oxyhaemoglobin becomes diamagnetic [6,7]. Electron paramagnetic resonance, another magnetism-based technique, has also revealed paramagnetism in other iron-containing proteins, such as cytochromes and transferrin [8].

In the case of the iron storage protein ferritin, the Fe atoms are not individually coordinated to the organic molecule but mineralised in the form of oxyhydroxide nanoparticles at the core of the protein [1]. From the magnetic point of view these nanoparticles behave as magnetic super-units in analogy to the individual magnetic ions in a paramagnet. This property is called *superparamagnetism*, which manifests itself by a static magnetic susceptibility also proportional to the reciprocal of the absolute temperature (1/T) in the same way as that of paramagnetism. Nevertheless, superparamagnetic nanoparticles can be differentiated from paramagnetic compounds by measuring the AC magnetic susceptibility, which is the alternating current (AC) variant of the static one. This technique offers in the same experiment two quantities, namely, the in-phase component (χ') and the out-of-phase component (χ''). It is χ'', and especially its temperature dependence profile $\chi''(T)$, which is a typical feature to look at for detecting magnetic nanoparticles and, hence, iron biomineralisation [9].

* Correspondence to: L. Gutiérrez, School of Physics M013, The University of Western Australia, 35 Stirling Hwy, Crawley, WA, 6009, Australia. Tel.: +61 864881132.
** Correspondence to: M. Vujić Spasić, University Hospital of Heidelberg, Department of Hematology, Immunology and Oncology and Molecular Medicine Partnership Unit, Im Neuenheimer Feld 350, 69120, Heidelberg, Germany. Tel.: +49 6221568839.
E-mail addresses: lucia.gutierrez@uwa.edu.au (L. Gutiérrez), vujic@embl.de (M. Vujić Spasić).
[1] Lucía Gutiérrez and Maja Vujić Spasić contributed equally to this work.

0925-4439/$ – see front matter © 2012 Elsevier B.V. All rights reserved.
doi:10.1016/j.bbadis.2012.03.008

Recently, magnetic techniques in conjunction with tissue ultrastructure analysis were applied to quantify ferritin iron and other mineral iron-containing species. Specifically, iron supplement drugs [10,11], magnetic resonance imaging contrast agents [12] or drug delivery magnetic nanoparticles [13] may sometimes coexist with ferritin iron in the same tissue. Since all these iron-containing species exhibit distinguishable contributions to the magnetic susceptibility, the separate quantification of the iron present in these different forms becomes a feasible option.

Given the fact that the adverse biological functions of iron strongly depend on its chemical form, there is a great need to investigate the chemical speciation of this element. This is particularly necessary in the case of (patho-)physiological conditions with dysregulated cellular and systemic iron homeostasis, such as iron overload and iron deficiency disorders that belong to the most common pathologies across the globe. In regard to genetic iron overload disorders, the most prevalent form is caused by mutations in the Hfe gene [14]. The hallmark of hereditary haemochromatosis (HH) is increased serum iron levels and tissue iron deposition that eventually lead to multiple organ failure/dysfunction if the disease remains untreated. Mice homozygous for the Hfe null allele, and more precisely mice with exclusive Hfe deficiency in hepatocytes, reflect the HH phenotype observed in humans confirming that Hfe-HH arises from a loss of hepatocytic Hfe function [15–17].

The chemical form of tissue iron, investigated in other iron overload diseases [18–20], has rarely been monitored in more detail than the bare elemental content in genetic models of HH [21]. Therefore, in this work we have applied AC magnetic susceptibility measurements along with sensitive assays for iron determination, such as elemental content from Inductively Coupled Plasma Atomic Emission Spectroscopy (ICP-AES) and non-heme iron analysis to address the qualitative and quantitative distribution of iron containing species.

2. Material and methods

2.1. Mice

Age (8–12 weeks old) and sex-matched wild type (WT) and Hfe-deficient ($Hfe^{-/-}$) mice raised on a C57BL/6 genetic background were used for the analysis [22]. All mice were born and housed in the SPF animal facility of the EMBL (European Molecular Biology Laboratory). They were maintained on a standard mouse diet containing 225 mg/kg iron (Teklad 2018 S; Harlan Winkelmann, Borchen, Germany) on average and a constant dark–light cycle and allowed continuous access to food. Mice were killed by CO_2 inhalation. All mouse breeding and animal experiments were approved by and in compliance with the guidelines of the Institutional Animal Care and Use Committee of the EMBL.

Duodenum, liver, spleen, kidney and heart tissues were collected from WT and $Hfe^{-/-}$ mice and immediately immersed into liquid nitrogen with subsequent storage at −80 °C until carrying out the magnetic characterisation procedures.

2.2. AC magnetic susceptibility characterisation

The magnetic characterisation was carried out in a Quantum Design MPMS-5S SQUID magnetometer with an AC option that provides the in-phase χ' and out-of-phase χ'' components of the magnetic susceptibility. The measurements were performed in the temperature range 1.8–300 K, with an AC frequency of 1 Hz and amplitude of 0.45 mT. Adsorbed oxygen that might alter the magnetic behaviour of the samples was checked and found to be absent in all of them. For the purpose of AC magnetic characterisation, mouse tissues were freeze-dried for 48 h in a Heto PowerDry PL3000 equipment and then transferred into gelatine capsule sample holders. The mass ranges of dry tissue used for the magnetic characterisation were: 125–160 mg for the liver tissues, 18–35 mg for the spleens, 110–150 mg for the duodenum pools, 65–68 mg for the heart pools and 81–98 mg for the kidney pools.

2.3. Quantification of paramagnetic and superparamagnetic iron species

As a standard of paramagnetic and superparamagnetic iron, human haemoglobin in dry state (Sigma-Aldrich) and mouse liver ferritin (≈2000 Fe atoms/ferritin molecule) [23], respectively, were used.

The quantification procedure follows previously proposed guidelines [12]. Briefly, to determine the concentration of superparamagnetic iron, i) the $\chi''(T)$ profile per mass of iron of the ferritin standard has been fitted by an analytical function, ii) then it is checked that the temperature of the $\chi''(T)$ maximum for a given tissue actually coincides with that of the ferritin standard and iii) a multiple of the $\chi''(T)$ continuous line profile of the standard is fitted (Levenberg–Marquardt algorithm) to the $\chi''(T)$ maxima of the tissues. The multiplication factor obtained for the best fit is the iron concentration in the tissue in a similar form as that of the ferritin core. The $\chi''(T)$ profile is used for this determination, as there are no contributions to the out-of phase susceptibility profile from paramagnetic species. The amount of paramagnetic iron in the tissues is calculated from the $\chi'(T)$ profile after the subtraction of the superparamagnetic iron contribution whose concentration has been previously determined from the $\chi''(T)$ profile.

The $\chi''(T)$ profile reflects a given size distribution of particles that have specific composition and crystalline structure. Therefore, biomineralised iron species different from those of the ferritin cores of the standard used will show a $\chi''(T)$ maximum with either a different location in temperature or a different shape. Speaking in these terms, the $\chi''(T)$ profile of the studied tissues, as it will be shown in the results section, closely resembled that of the ferritin standard, indicating a very similar iron biomineralisation. Note that whether or not the biomineralised iron particles are actually contained within intact ferritin protein shells is something that cannot be determined from the magnetic measurements. Therefore, for the purpose of consistency, in what follows, this superparamagnetic species observed in the tissue samples will be called ferritin-like iron.

2.4. Elemental analysis

The elemental analysis of all freeze-dried tissues was performed by ICP-AES after an acid microwave digestion using 4:1 (v/v) 65% HNO_3 (w/v) and 30% H_2O_2 (w/v). For elemental analysis, as well as for magnetic determinations, the livers and spleens of each genotype/gender were analysed in duplicates, duodenum was characterised in pools from six individual mice, and kidneys and hearts in duplicate pools from three individuals each.

In addition to iron, Zn, Co, Ni, Mn, Cu and P were measured in all samples by ICP-AES. The content of elements with potentially marked magnetism was negligible in all the tissues, enabling us to interpret the AC magnetic susceptibility results as only respective to iron.

2.5. Measurements of tissue nonheme iron content

The nonheme iron content of the tissues was measured by the method previously described by Torrance and Bothwell [24]. Briefly, tissues were dried (72 h/42 °C), and digested in 10% TCA (w/v)/10% HCl (w/v) (48 h/65 °C). Tissue debris was pelleted by centrifugation (13,000 rpm/5 min). 20 µl of 10× diluted supernatant were added to 100 µl of chromogenic solution (6 M Na acetate/0.01%(w/v) bathophenanthroline-disulfonic acid/0.1% (w/v) thioglycolic acid) in a 96-well plate and incubated for 10 min at room temperature. Absorbance (535 nm) was measured in a photometer (SpectramaxPlus, Molecular Devices). The iron content was calculated using serial

dilution of an iron-standard (iron atomic absorption standard solution, Sigma-Aldrich).

2.6. Statistical analysis

Data are shown as mean values ± standard deviation (SD). Statistical analysis was performed using Student *t*-test, and p values <0.05 (*), <0.025 (**) and <0.0005 (***) are considered as significant.

3. Results and discussion

3.1. Magnetic susceptibility of ferritin and haemoglobin

To standardise the magnetic analysis we initially characterised the magnetic behaviour of purified single iron-containing proteins such as a sample of commercial human haemoglobin and a sample of mouse liver ferritin [23]. The magnetic susceptibility of haemoglobin illustrates the concept of *paramagnetic* iron because $\chi'(T)$ follows the Curie law (Fig. 1A), while χ'' is zero under the experimental resolution in the whole temperature range (Fig. 1B). Ferritin, on the other hand, illustrates *superparamagnetic* iron behaviour because $\chi'(T)$ also follows the Curie law at high temperatures, peaks slightly above 10 K and decreases with decreasing temperature (Fig. 1A). The single $\chi''(T)$ bell-shaped maximum, with the same magnetic origin as that of $\chi'(T)$, between about 8 K and 10 K, shown by ferritin (Fig. 1B) is a hallmark of ferritin-like iron.

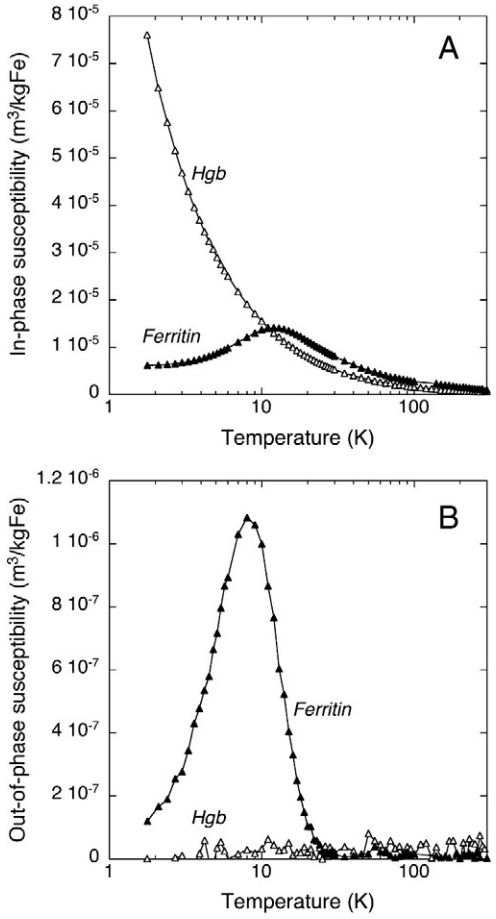

Fig. 1. AC susceptibility of ferritin and haemoglobin. (A) Temperature dependence of the in-phase susceptibility component, per mass of elemental Fe, of human haemoglobin (Hgb) and mouse liver ferritin (Ferritin) to illustrate ionic paramagnetism and nanoparticle superparamagnetism respectively. (B) Temperature dependence of the out-of-phase susceptibility component of the same molecules. The shape and location in temperature of the bell-shaped maximum of ferritin constitute the exclusive marker for nanoparticulate mineral iron at the core of this molecule. In both figures, the line has been obtained by joining the experimental points.

3.2. Magnetic susceptibility of tissues from Hfe$^{-/-}$ mice

The two components of the AC susceptibility, χ' and χ'', of liver tissues from Hfe$^{-/-}$ and wild-type mice are depicted in Fig. 2. The out-of-phase susceptibility (Fig. 2B) is zero within the experimental sensitivity above 40 K, but shows a bell-shaped maximum between about 8 K and 10 K indicative of ferritin-like iron. At the maximum, the height of the $\chi''(T)$ curve is proportional to the amount of ferritin-like iron, provided, as in this case, that the temperature of this maximum corresponds to that of the ferritin standard.

Given that for purified ferritin χ' decreases at low temperatures (Fig. 1A), the low temperature $\chi'(T)$ rise, with no associated visible feature in $\chi''(T)$, shown in Fig. 2A indicates the presence of additional paramagnetic iron in the liver tissues. This iron species can only be discerned at low temperatures, as its paramagnetic Curie law susceptibility is confounded with the superparamagnetic one at high temperatures.

The height of the out-of-phase susceptibility maximum corresponding to liver tissues of Hfe$^{-/-}$ mice is significantly higher than for the WT animals. This indicates that Hfe-deficient livers accumulate iron predominantly in the form of ferritin-like iron (Fig. 2B). Furthermore Hfe$^{-/-}$ females show higher ferritin-like iron levels than males, similar to the sex-specific distribution observed in WT mice.

The magnetic analysis of spleen tissues reveals a remarkably high $\chi''(T)$ maxima for the WT mice compared to Hfe$^{-/-}$ mice (Fig. 2D), implying an iron-deficient phenotype of the spleen (i.e. of macrophages) in Hfe$^{-/-}$ mice. In particular, the female WT and Hfe$^{-/-}$ mice show a higher $\chi''(T)$ maximum than the male counterparts, suggestive of a higher amount of ferritin-like iron present in these tissues.

The paramagnetic tail that is observed in $\chi'(T)$ (Fig. 2A and C) of the liver and spleen samples indicates the presence of paramagnetic iron-containing species, very likely in the form of haemoglobin.

Preliminary analysis of magnetic susceptibility of duodenum, kidney and heart tissues from individual mice showed measurements within the background noise (data not shown). To increase the quality of the measurements we pooled the respective tissues from WT and Hfe$^{-/-}$ mice and the results of the magnetic analysis are shown in Fig. 3. The observation of $\chi''(T)$ maxima around 10 K indicates the presence of ferritin-like iron in the duodenum (Fig. 3B). Both WT and Hfe$^{-/-}$ animals show a similar amount of ferritin-like iron in duodenal tissues, although a tendency to accumulate more iron is observed in male WT compared to Hfe$^{-/-}$ mice. The amount of paramagnetic iron appears similar for all the analysed groups (Fig. 3A).

The magnetic susceptibility of kidney and heart tissues indicates that $\chi''(T)$ is practically zero within the intrinsic noise level (Fig. 3D, F), suggesting that the amount of ferritin-like iron is below the detection limits of this technique. Those limits, determined from the experimental noise, can though be used to estimate the upper limit for the possible ferritin-like iron concentration. The content of paramagnetic iron in kidneys and hearts seems not to differ significantly between the genotypes (Fig. 3C, E).

3.3. Comparative analysis of iron-containing species in Hfe-deficient tissues

We next compared the results obtained from magnetic susceptibility measurements with those obtained from other well-established techniques such as ICP-AES and nonheme iron content (Fig. 4).

Analysis of the hepatic iron content using ICP-AES reveals significantly increased iron levels in Hfe$^{-/-}$ mice compared to WT controls, further indicating that more iron is present in females than in males.

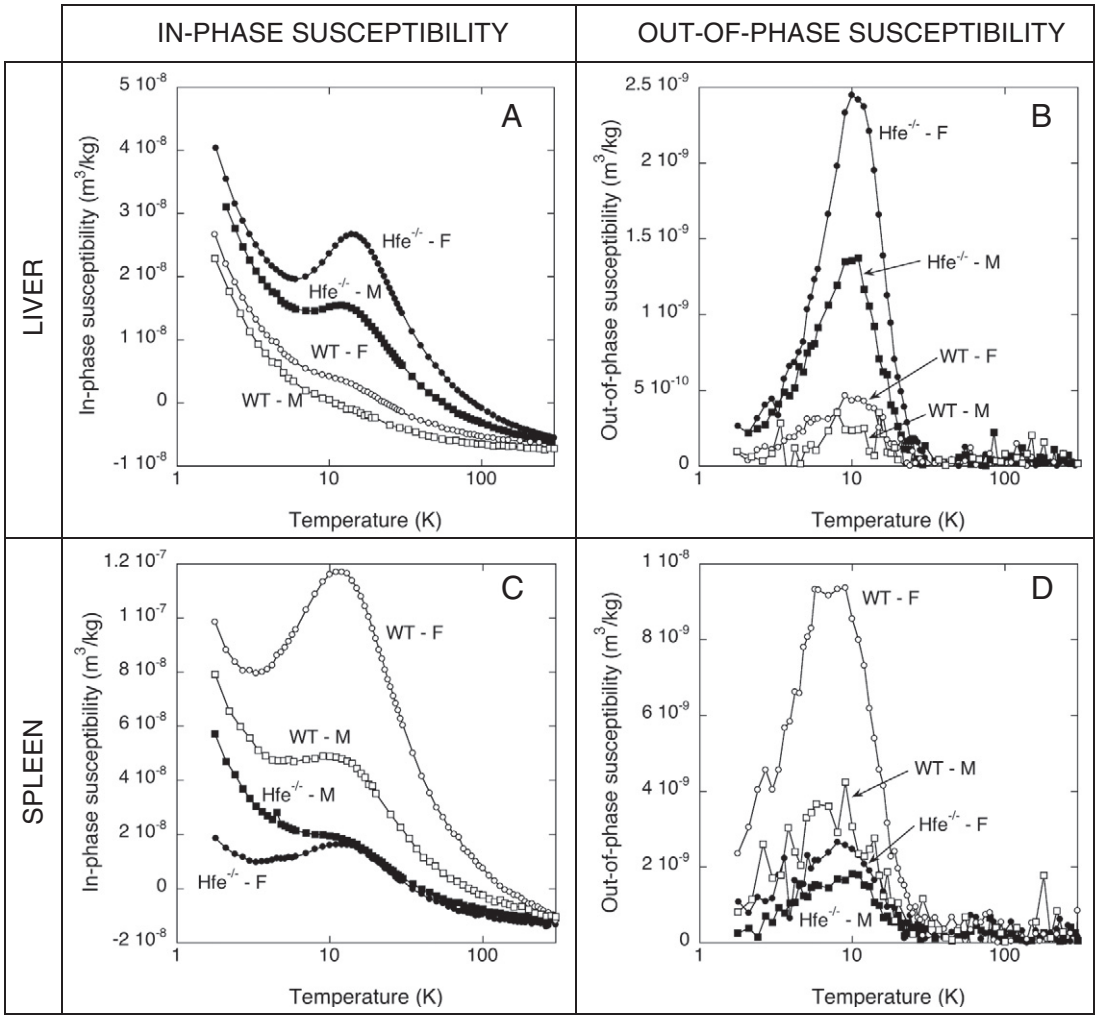

Fig. 2. AC susceptibility of liver and spleen tissues of $Hfe^{-/-}$ mice. (A) and (B) Temperature dependence of the in-phase (χ') and out-of-phase (χ'') components of the susceptibility per mass of sample, of freeze-dried liver tissues. (C) and (D) χ' (T) and χ'' (T) per mass of sample, of freeze-dried spleen tissues. In all the panels, each curve corresponds to a representative individual (F = female, M = male) of WT and $Hfe^{-/-}$ mice.

Importantly, there were no significant differences in the concentration of Cu, Zn or P between WT and KO animals, and the amount of Co, Mn and Ni was under the detection limits of the technique.

The values of total elemental iron (Fig. 4A) mirror those of ferritin-like iron in the liver (Fig. 4B) suggesting that most of the iron in the liver is stored in the same biomineralised form as in the ferritin inorganic nucleus. This result is consistent with the low values of paramagnetic iron, shown in Fig. 4C and D. In particular, the sum of the ferritin-like iron (Fig. 4B) and paramagnetic iron (Fig. 4D) should be similar to the total iron determined by elemental analysis (Fig. 4A).

The difference in the hepatic nonheme iron content between WT and $Hfe^{-/-}$ mice (Fig. 4E) shows the same trend as the elemental and ferritin-like iron.

These data reveal an excellent agreement among the three techniques used to quantify different iron-containing species in the liver. Interestingly, in the spleen, the non-heme iron content is significantly lower than the total iron and ferritin-like iron (Fig. 4A, B, E). Thus, the splenic iron content is characterised by the presence of ferritin-like iron, total iron (as well as ferritin and nonheme iron) that is significantly lower in spleens of $Hfe^{-/-}$ mice than in WT mice, and a significant portion of paramagnetic iron compared to the liver, likely in the form of haemoglobin.

It is interesting to note that serum ferritin in Hfe-deficient mice is significantly higher than in control mice (102.63 ± 9.29 μg/L vs. 42.2 ± 4.56 μg/L, $p < 0.005$) suggesting that a correlation between increased tissue iron-ferritin and serum ferritin levels exists. It is likely that hepatocytes may be a source of serum ferritin in Hfe-HH. As the serum ferritin generally reflects body iron status our results would support the notion that serum ferritin may reflect the hepatocytic iron status in Hfe-HH. By contrast, non-Hfe iron overload disorders may be characterised by the presence of ferritin derived preferentially from macrophages, as previously observed in $Irp^{-/-}$ mice [23].

The concentration of paramagnetic iron is not significantly different between WT and $Hfe^{-/-}$ mice or between genders for the same tissue ($p > 0.09$). The observation that paramagnetic iron (an important representative of nonferritin iron) tends to be enhanced in the spleen in comparison to the liver (Fig. 4C) appears in agreement with the presence of haemoglobin in splenic macrophages from recycled red blood cells, given the specific biological function of this organ.

4. Conclusions

With this work we present a thorough and interdisciplinary study on the iron speciation in different tissues from a murine model of Hfe-haemochromatosis. Results from the qualitative and quantitative magnetic determination of different iron-containing forms are consistent with well-established analytical methods. The magnetic measurements are quite suitable and selective for this purpose as the biogenic iron-containing chemical species show magnetic features

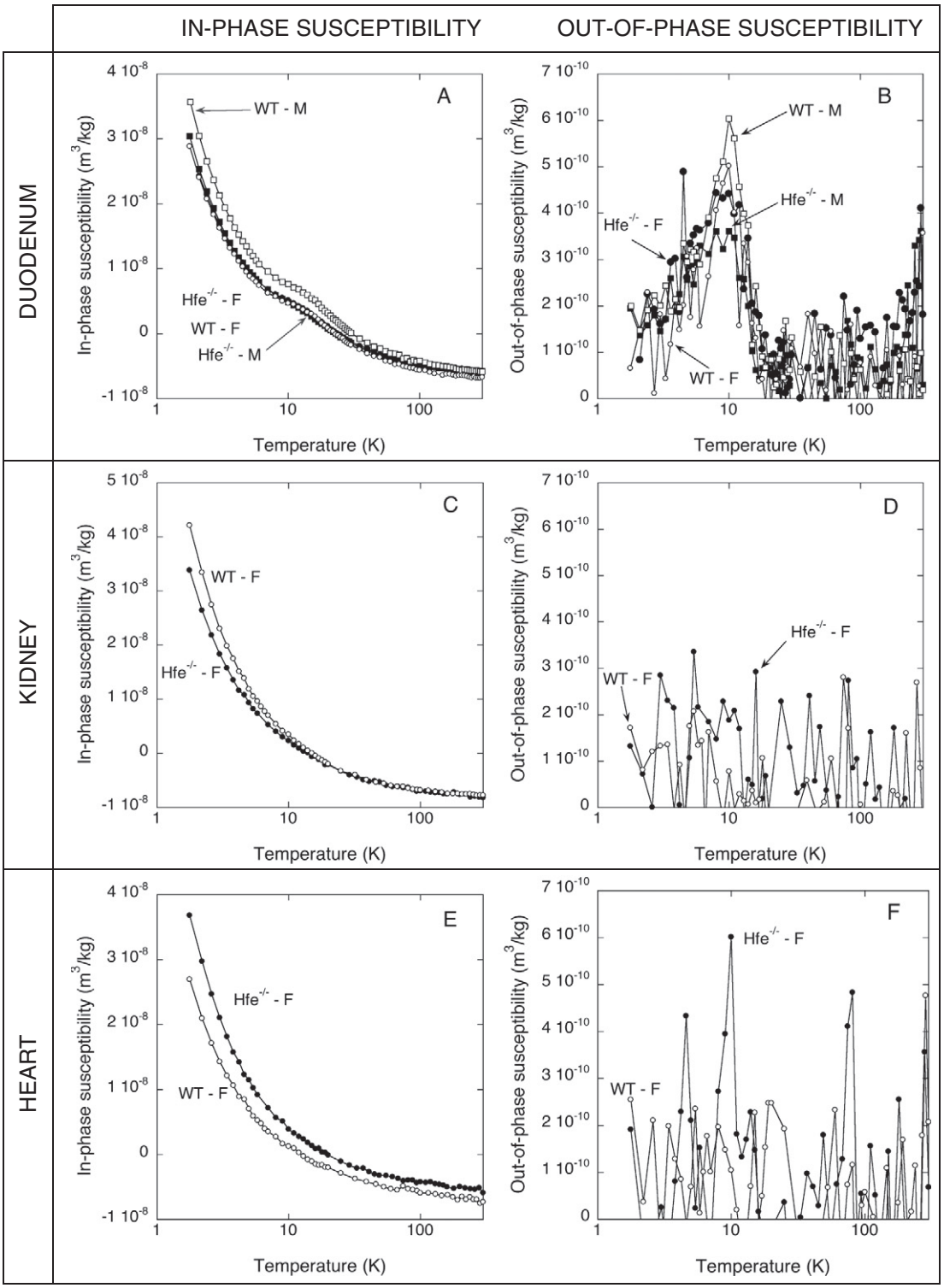

Fig. 3. AC susceptibility of duodenum, kidney and heart tissues of $Hfe^{-/-}$ mice. (A) and (B) Temperature dependence of the in-phase (χ') and out-of-phase (χ'') components of the susceptibility, per mass of sample, of freeze-dried duodenum tissues. (C) and (D) χ' (T) and χ'' (T) per mass of sample, of freeze-dried kidney tissues. (E) and (F) χ' (T) and χ'' (T) per mass of sample, of freeze-dried heart tissues. In all of the panels, and due to their low magnetic signal to noise ratio, data correspond to age- and sex-matched (F = female, M = male) WT and $Hfe^{-/-}$ mice tissue pools.

at temperatures different from those of other nanoparticulate iron-containing compounds (e.g. iron dextran, iron sucrose [25,26], etc.) that are often administered to mice for the purpose of studying the regulation of cellular/systemic iron homeostasis.

With these measurements we have found that most iron in $Hfe^{-/-}$ mice tissues is in the form of ferritin-like iron, while different proportions of the less abundant non-ferritin iron may be related to the biological function of each organ.

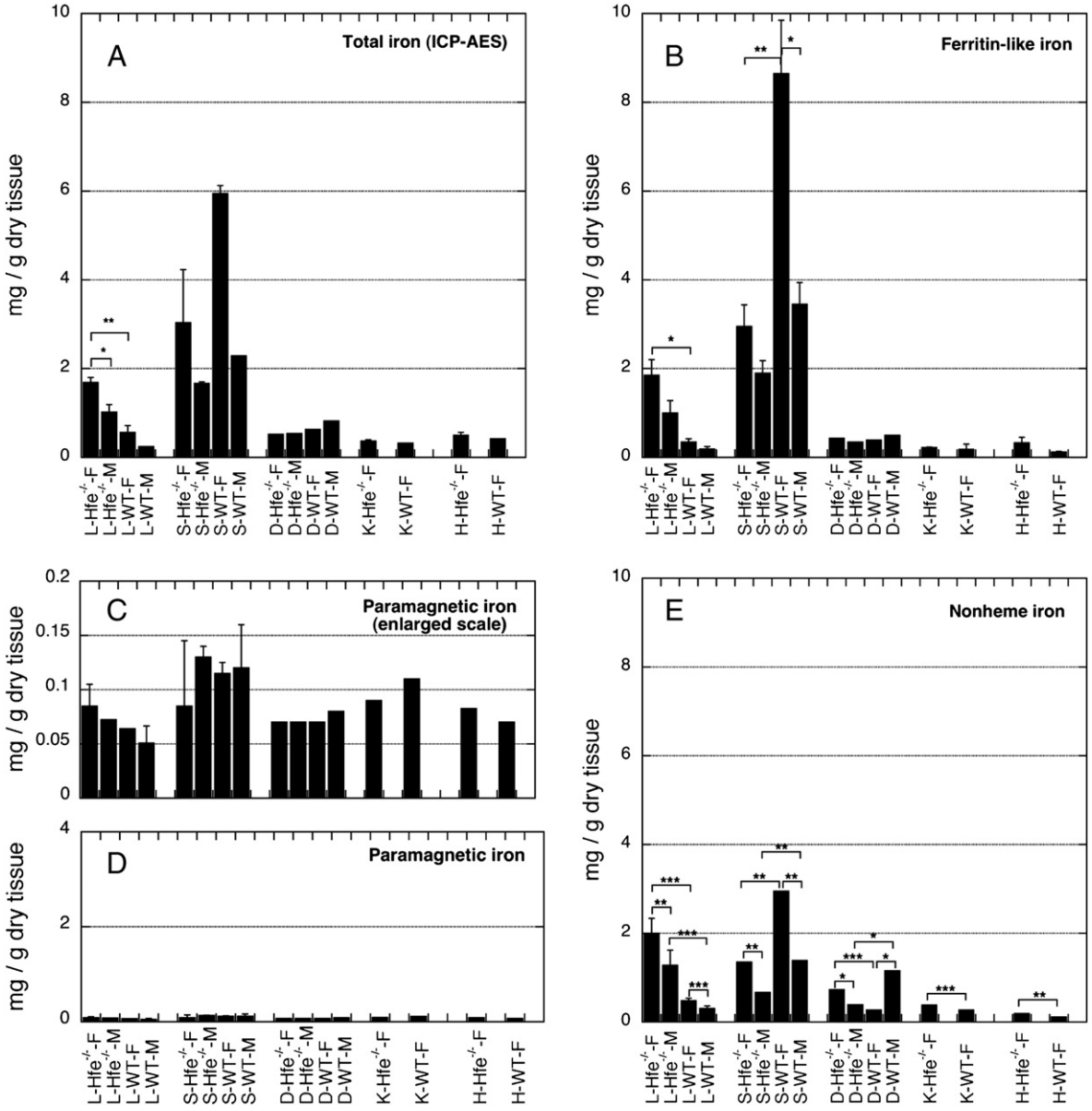

Fig. 4. Iron speciation in tissues from $Hfe^{-/-}$ mice. Iron contents in the different chemical forms and tissues for the different genotypes/genders (L = liver, S = spleen, D = duodenum, K = kidney, H = heart, F = female, M = male). (A) Total elemental iron determined by ICP-AES. (B) Magnetically determined ferritin-like iron. (C) and (D) Magnetically determined paramagnetic iron; these two plots have identical horizontal labelling. (E) Non-heme iron determined by the Torrance–Bothwell method. All the panels, with the exception of (C), use the same iron concentration scale in order to facilitate the comparison. With the exception of the pool samples, the error bars correspond to the standard deviation of the quantitative determinations among the replicates (* $p<0.05$; ** $p<0.025$, *** $p<0.0005$). Ferritin-like iron contents for kidneys and hearts should be understood as upper limit values (see explanation in Section 3.2 of the text).

Given the role of iron in many diseases, the development of protocols to study the iron speciation in tissues may be a key parameter in the study of the progression of diseases or the development of new diagnostic techniques.

Acknowledgements

The authors thank L. Cohen and E. Meyron-Holtz for providing ferritin standard samples and Mike House for his critical reading of the manuscript. The authors would like to thank the staff of the EMBL laboratory animal facility for their expert support and the Hopp Stiftung. This work was supported by the Instituto de Salud Carlos III [PI060549 to F.J.L.], the BMBF [HepatoSys and Virtual Liver — 0315761, eRARE — 01GM1005 to M.U.M.] and by the University of Heidelberg Award [to M.V.S.]. L.G. receives a Sara Borrell postdoctoral contract from the Spanish ISCIII-MSPS [CD09/00030].

References

[1] R.R. Crichton, Inorganic Biochemistry of Iron Metabolism, John Wiley and Sons Ltd, Chichester, England, 2001.
[2] G.M. Brittenham, D.E. Farrell, J.W. Harris, E.S. Feldman, E.H. Danish, W.A. Muir, J.H. Tripp, E.M. Bellon, Magnetic-susceptibility measurement of human iron stores, N. Engl. J. Med. 307 (1982) 1671–1675.
[3] L. Pauling, C.D. Coryell, The magnetic properties and structure of hemoglobin, oxyhemoglobin and carbonmonoxyhemoglobin, Proc. Natl. Acad. Sci. U. S. A. 22 (1936) 210–216.
[4] C.D. Coryell, F. Stitt, L. Pauling, The magnetic properties and structure of ferrihemoglobin (methemoghbin) and some of its compounds, J. Am. Chem. Soc. 59 (1937) 633–642.
[5] D.S. Taylor, The magnetic properties of myoglobin and ferrimyoglobin, and their bearing on the problem of the existence of magnetic interactions in hemoglobin, J. Am. Chem. Soc. 61 (1939) 2150–2154.
[6] L. Pauling, Magnetic properties and structure of oxyhemoglobin, Proc. Natl. Acad. Sci. U. S. A. 74 (1977) 2612–2613.
[7] M. Cerdonio, S. Morante, D. Torresani, S. Vitale, A. DeYoung, R.W. Noble, Reexamination of the evidence for paramagnetism in oxy- and carbonmonoxyhemoglobins, Proc. Natl. Acad. Sci. U. S. A. 82 (1985) 102–103.

[8] M. Ubbink, J.A.R. Worrall, G.W. Canters, E.J.J. Groenen, M. Huber, Paramagnetic resonance of biological metal centers, Annu. Rev. Biophys. Biomol. Struct. 31 (2002) 393–422.
[9] F.J. Lázaro, L. Gutiérrez, A.R. Abadía, M.S. Romero, A. López, Biological tissue magnetism in the frame of iron overload diseases, J. Magn. Magn. Mater. 316 (2007) 126–131.
[10] F.J. Lázaro, A.R. Abadía, M.S. Romero, L. Gutiérrez, J. Lázaro, M.P. Morales, Magnetic characterisation of rat muscle tissues after subcutaneous iron dextran injection, Biochim. Biophys. Acta Mol. Basis Dis. 1740 (2005) 434–445.
[11] L. Gutiérrez, F.J. Lázaro, A.R. Abadía, M.S. Romero, C. Quintana, M.P. Morales, C. Patiño, R. Arranz, Bioinorganic transformations of liver iron deposits observed by tissue magnetic characterisation in a rat model, J. Inorg. Biochem. 100 (2006) 1790–1799.
[12] A. López, L. Gutiérrez, F.J. Lázaro, The role of dipolar interaction in the quantitative determination of particulate magnetic carriers in biological tissues, Phys. Med. Biol. 52 (2007) 5043–5056.
[13] L. Gutiérrez, R. Mejías, D.F. Barber, S. Veintemillas-Verdaguer, C.J. Serna, F.J. Lázaro, M.P. Morales, Ac magnetic susceptibility study of in vivo nanoparticle biodistribution, J. Phys. D Appl. Phys. 44 (2011) 255002–255010.
[14] J.N. Feder, A. Gnirke, W. Thomas, Z. Tsuchihashi, D.A. Ruddy, A. Basava, F. Dormishian, R. Domingo Jr., J.N. Feder, A. Gnirke, W. Thomas, Z. Tsuchihashi, D.A. Ruddy, A. Basava, F. Dormishian, R. Domingo Jr., M.C. Ellis, A. Fullan, L.M. Hinton, N.L. Jones, B.E. Kimmel, G.S. Kronmal, P. Lauer, V.K. Lee, D.B. Loeb, F.A. Mapa, E. McClelland, N.C. Meyer, G.A. Mintier, N. Moeller, T. Moore, E. Morikang, C.E. Prass, L. Quintana, S.M. Starnes, R.C. Schatzman, K.J. Brunke, D.T. Drayna, N.J. Risch, B.R. Bacon, R.K. Wolff, A novel MHC class I-like gene is mutated in patients with hereditary haemochromatosis, Nat. Genet. 13 (1996) 399–408.
[15] K.R. Bridle, D.M. Frazer, S.J. Wilkins, J.L. Dixon, D.M. Purdie, D.H. Crawford, V.N. Subramaniam, L.W. Powell, G.J. Anderson, G.A. Ramm, Disrupted hepcidin regulation in HFE-associated haemochromatosis and the liver as a regulator of body iron homoeostasis, Lancet 361 (2003) 669–673.
[16] M.U. Muckenthaler, C.N. Roy, A.O. Custodio, B. Minana, J. de Graaf, L.K. Montross, N.C. Andrews, M.W. Hentze, Regulatory defects in liver and intestine implicate abnormal hepcidin and Cybrd1 expression in mouse hemochromatosis, Nat. Genet. 34 (2003) 102–107.
[17] M. Vujic Spasić, J. Kiss, T. Herrmann, B. Galy, S. Martinache, J. Stolte, H.J. Grone, W. Stremmel, M.W. Hentze, M.U. Muckenthaler, Hfe acts in hepatocytes to prevent hemochromatosis, Cell Metab. 7 (2008) 173–178.
[18] T.G. St Pierre, D.P.E. Dickson, J.K. Kirkwood, R.J. Ward, T.J. Peters, A Mössbauer spectroscopic study of the form of iron in iron overload, Biochim. Biophys. Acta 924 (1987) 447–451.
[19] R.J. Ward, M. Ramsey, D.P.E. Dickson, C. Hunt, T. Douglas, S. Mann, F. Aouad, T.J. Peters, R.R. Crichton, Further characterisation of haemosiderin in iron-overloaded tissues, Eur. J. Biochem. 225 (1994) 187–194.
[20] W. Chua-anusorn, J. Webb, D.J. Macey, P. de la Motte Hall, T.G. St. Pierre, The effect of prolonged iron loading on the chemical form of iron oxide deposits in rat liver and spleen, Biochim. Biophys. Acta 1454 (1999) 191–200.
[21] L. Gutiérrez, C. Quintana, C. Patiño, J. Bueno, H. Coppin, M.P. Roth, F.J. Lázaro, Iron speciation study in Hfe knockout mice tissues: magnetic and ultrastructural characterisation, Biochim. Biophys. Acta Mol. Basis Dis. 1792 (2009) 541–547.
[22] M. Vujic Spasić, J. Kiss, T. Herrmann, R. Kessler, J. Stolte, B. Galy, B. Rathkolb, E. Wolf, W. Stremmel, M.W. Hentze, M.U. Muckenthaler, Physiologic systemic iron metabolism in mice deficient for duodenal Hfe, Blood 109 (2007) 4511–4517.
[23] L.A. Cohen, L. Gutiérrez, A. Weiss, Y. Leichtmann-Bardoogo, D. Zhang, D.R. Crooks, R. Sougrat, A. Morgenstern, B. Galy, M.W. Hentze, F.J. Lázaro, T.A. Rouault, E.G. Meyron-Holtz, Serum ferritin is derived primarily from macrophages through a nonclassical secretory pathway, Blood 116 (2010) 1574–1584.
[24] J.D. Torrance, T.H. Bothwell, in: J.D. Cook (Ed.), Methods in Hematology, Churchill Livingston Press, New York, 1980, pp. 104–109.
[25] F.J. Lázaro, A. Larrea, A.R. Abadía, Magnetostructural study of iron-dextran, J. Magn. Magn. Mater. 257 (2003) 346–354.
[26] L. Gutiérrez, M.P. Morales, F.J. Lázaro, Magnetostructural study of iron sucrose, J. Magn. Magn. Mater. 293 (2005) 69–74.